

Research Progress on Flow Behavior and Constitutive Models of γ -TiAl Alloys Deformed at Elevated Temperature

Xu Runrun, Li Miaoquan, Li Hong

Northwestern Polytechnical University, Xi'an 710072, China

Abstract: γ -TiAl alloys with a low density and a high specific stiffness are preferred structural materials for weight saving of aircraft engines. The present paper deeply reviewed the flow behavior and constitutive equations of γ -TiAl alloys compressed at elevated temperature. Deformation processing parameters, deformation history and adjusted preheating treatment, chemical composition and initial microstructures are the main factors that determine the flow behavior of γ -TiAl alloys compressed at elevated temperature. The constitutive models describing flow stress-strain curves are segmented into genres, such as empirical models, models coupled with different softening mechanisms, and models about deformation mechanisms. The Arrhenius model and H-S model were deeply discussed. Also, constitutive model including softening mechanism and models involving deformation mechanisms were summarized and analyzed. It can be predicted that the emphasis on further research in γ -TiAl alloys is to establish constitutive models involving multiphase coordinated deformation mechanisms.

Key words: γ -TiAl alloys; high temperature deformation; flow behavior; constitutive models

γ -TiAl alloys, for their excellent properties such as low density and outstanding specific stiffness, are potential materials for replacing Ti alloys and Ni-base superalloys in aerospace applications^[1-7]. Application of γ -TiAl alloys would be beneficial for engine to reduce weight and to raise fuel efficiency^[3, 4, 8-10]. Ti-48Al-2Nb-2Cr, which helps to reduce weight of engines^[11], has been employed to produce low pressure turbine blades of LEAPTM engines running on Boeing's B737MAX etc^[1,3]. Currently, γ -TiAl alloys have been introduced into service by many companies including GE, MTU and MW Racing. Besides, Rolls-Royce plans to employ γ -TiAl alloys for aero applications. As Janschek^[12] said, in order to realize this plan, about 900 pieces of blades of high pressure compressor are forged for their experimental engine E3E.

An attractive progress in weight reduction for aero engines is achieved by implementation of γ -TiAl alloys. However, stumbling blocks for thermomechanical processing are their intrinsic brittleness and narrowing tem-

perature window on industrial scale^[3,13,14]. Physical simulation method is a common way to get a thorough understanding of flow behavior of γ -TiAl alloys at elevated temperature^[15]. In addition, thermal simulation compression test can be taken as a reference for the numerical simulation of forging γ -TiAl alloys. Furthermore, through the thermal simulation compression test, suitable loads of forging equipment and optimum processing parameters can be determined.

In this paper, based on flow behavior of γ -TiAl alloys compressed at elevated temperature, the features and influential factors of flow stress-strain curves were primarily analyzed. Besides, various constitutive models describing the instant response of γ -TiAl alloys to external load were compared in detail.

1 Flow Behavior of γ -TiAl Alloys Deformed at Elevated Temperature

1.1 Flow stress-strain curves

Received date: May 21, 2018

Foundation item: National Natural Science Foundation of China (51505386); Fundamental Research Funds for the Central Universities (3102017gx06003)

Corresponding author: Li Miaoquan, Ph. D., Professor, School of Materials Science and Engineering, Northwestern Polytechnical University, Xi'an 710072, P. R. China, Tel: 0086-29-88460328, E-mail: honeyqli@nwpu.edu.cn

Copyright © 2019, Northwest Institute for Nonferrous Metal Research. Published by Science Press. All rights reserved.

Flow stress-strain curves reflect the instantaneous response of microstructure to applied loads during the compression of materials. The response is associated with deformation processing parameters. Also, it is influenced by chemical composition and original microstructure.

The typical flow stress-strain curve for isothermal compression of γ -TiAl alloys is presented in

Fig.1. As seen in

Fig.1, features of flow behavior are shown as follows: in the initial stage of deformation, the flow stress of γ -TiAl alloys drastically increases until peak stress (σ_p) is achieved; and then, the flow stress falls, so does the amplitude of flow stress. The saturation stress (σ_{ss}) is reached if the deformation continues. The flow stress-strain curve of γ -TiAl alloys is mainly softened by dynamic recrystallization (DRX), which makes the flow stress peaked.

1.1.1 Effect of work hardening and flow softening

Flow stress decreases with increasing the deformation temperature or decreasing the strain rate, as shown in Fig.2^[16]. Flow stress-strain curves are a macroscopic manifestation of competition between work hardening and flow softening. Work hardening is dominant at the first stage when dislocation density increases with strain and dislocations are hindered by grain boundaries and other barriers. Flow softening, associated with a mass of interactions between dislocations, results from dynamic recrystallization (DRX), dynamic recovery (DRV) and adiabatic heat^[17]. Flow softening extent ($\Delta\sigma = \sigma_p - \sigma_{ss}$) reflects the offset of work hardening and flow softening. Effect of deformation temperature and strain rate on flow softening extent is presented in Fig.3. Flow softening extent decreases with increasing the deformation temperature or decreasing the strain rate, which implies that softening mechanisms are less effective and can be attributed to DRX during isothermal compression^[18].

Effect of strain on flow stress of γ -TiAl alloys is reflected through work hardening rate ($\theta = \partial\sigma / \partial\varepsilon$), as shown in Fig.4. Work hardening rate rapidly declines with increasing the strain, and declines slightly when DRX occurs. Work hardening

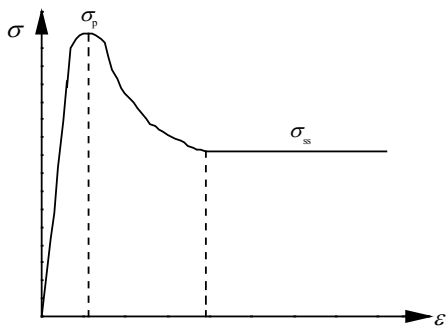


Fig.1 Typical flow stress-strain curve of γ -TiAl alloys

is predominant until flow stress peaked. Afterwards, work hardening rate becomes negative, which means that softening mechanism plays a leading role. Then, work hardening rate keeps declining until the valley touched, which implies that flow softening induced by DRX is sharper than that at any time. Subsequently, work hardening rate gradually increases until it approaches to 0, as exhibited in Fig.4. The strain dependence of work hardening rate reflects the strain dependence of dislocation density and dislocation interaction. Dislocation is accumulated by work hardening and annihilated by DRV and DRX. Cheng et al^[19] claimed that contribution of DRV to the dislocation annihilation of γ -TiAl alloys can be neglected.

1.1.2 Effect of deformation history and adjusted preheating treatment

To some extent, γ -TiAl alloys, which were subjected to pre-deformation or preheating treatment, exhibit preferable hot deformability owing to a decline in internal stress and defaults. Besides, grain sizes and microstructure morphology are altered by deformation history and advance heating treatment^[20], which decreases the deformation resistance of γ -TiAl alloys^[21]. Seetharaman et al^[13] assessed the influence of preheating temperature and deformation temperature on Ti-45.5Al-2Nb-2-Cr. The results showed that the higher the preheating temperature, the sharper the peak stress and the larger the flow softening extent, due to the increased size and fraction of lamellar colony. However, this phenomenon is

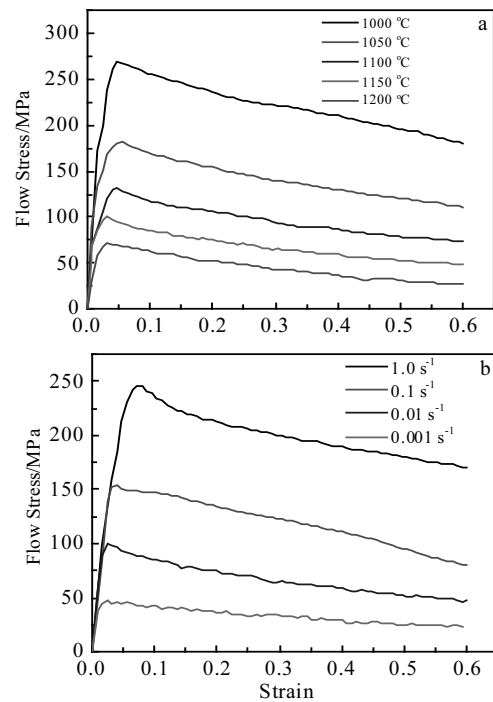


Fig.2 Flow stress-strain curves of Ti-45Al-8Nb-2Cr-2Mn at a strain rate of 0.01 s (a) and a deformation temperature of 1150 °C (b)^[16]

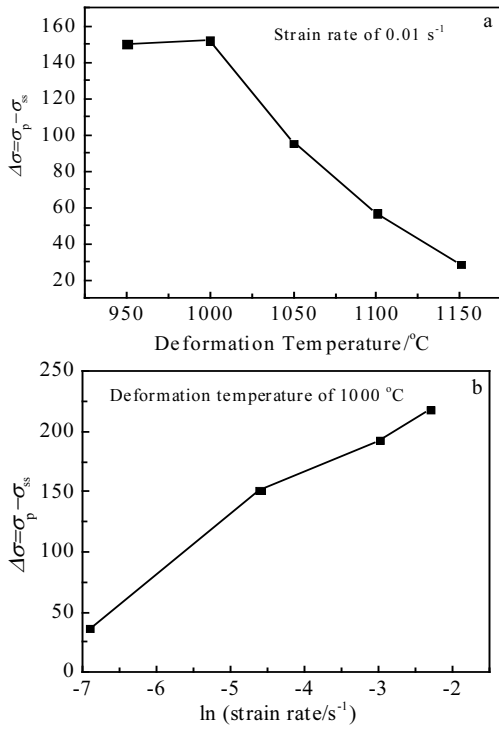


Fig.3 Effect of deformation temperature (a) and strain rate (b) on flow softening extent of Ti-47Al-2Nb-2Cr^[18]

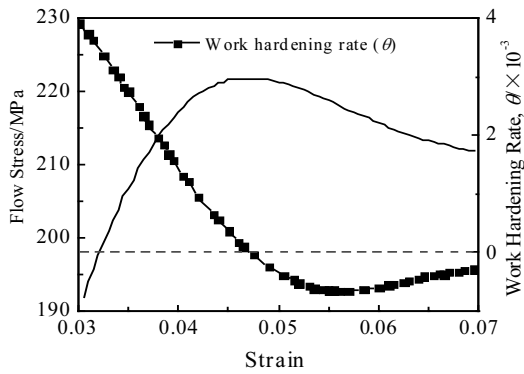


Fig.4 Effect of strain on flow stress and work hardening rate of Ti-42Al-8Nb-0.2W-0.1Y (deformation temperature 1100 °C, strain rate 0.01 s⁻¹)^[19]

weakened with increasing the deformation temperature and lowering the strain rate, as most short-range glide obstacles are removed^[22]. Paul et al^[23] claimed that the short-range obstacles (debris and dipoles) caused work hardening to be sensitive to deformation processing parameters.

The effect of deformation frequency, interval of deformation and temperature drop on flow stress of Ti-45.3Al-2Cr-2Nb-0.1B was assessed, which are attributed to DRX and DRV^[24]. Fig.5 shows the flow stress curves of γ -TiAl alloy

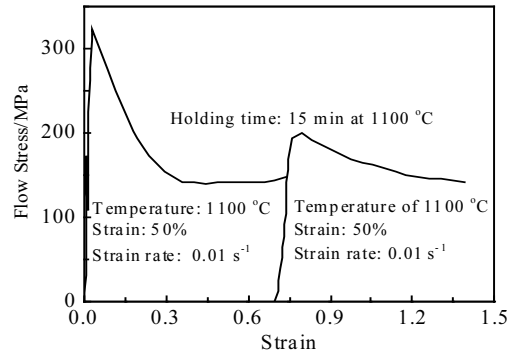


Fig.5 Flow stress-strain curve of Ti-47Al-2Cr-1Nb subjected to double compression at elevated temperature^[25]

which was deformed at a deformation temperature of 1100 °C, a strain rate of 0.01 s⁻¹, and a height reduction of 50% with an interval of 15 min at the same temperature. As shown in Fig.5, the flow stress decreases by about 35.9%, which is attributed to the DRX of γ grain and static balling of lamellae during the interval^[25].

1.1.3 Effect of elements

In order to screen out γ -TiAl alloy compositions meeting service requirements of aeronautic materials and to show balanced properties between service and hot workability, it is necessary to clarify the effect of elements on the microstructure morphology and high-temperature properties of γ -TiAl alloys. According to alloy design strategy^[26, 27], there are two types of elements: aluminum and other alloying elements. The influence of elements on deformation behavior of γ -TiAl alloys is elucidated below.

Different contents of Al alter solidification paths of γ -TiAl alloys, which results in variation in microstructure morphology and phase fractions, thus leading to various machinability properties at elevated temperatures^[28]. Imayev et al^[29] announced that as the Al content increases, the flow stress of binary γ -TiAl alloy gradually decreases, which is related to the increase of volume fraction of α_2 phase^[30]. For ternary γ -TiAl alloys (Al<45 at%), flow stress declines with increasing the Al contents, due to the increase in the volume fraction of β_0 phase^[8].

Also, alloying elements are substantial for flow stress of γ -TiAl alloys compressed at elevated temperature. Proper addition of Nb, Mo, Ta and W elements in γ -TiAl alloys is beneficial for β_0 phase^[31]. Trace addition of Y, B, C and Si elements is conducive to diminishing grain size and refining lamellar spacing^[26, 32, 33]. Mn would contribute to the twinning in γ -TiAl alloys^[34]. Above mentioned elements improve hot workability of γ -TiAl alloys. Nazarova et al^[35] announced that hot workability and ductility of Ti-45Al-5Fe(-5Nb) at room temperature can be improved by $\tau_2(\text{Al}_2\text{FeTi})$ phase which is induced by adding Fe elements.

Besides, hydrogen is also beneficial for hot workability of γ -TiAl alloys, which yields a 35% decrease in peak stress of Ti-46Al-2V-1Cr-0.3Ni^[17]. However, there are some divergences of specific effect of hydrogen on γ -TiAl alloys' hot workability. Hydrogen is beneficial for DRX of γ phase, dislocation sliding and twinning, or stabilizing β_0 phase^[17, 36]. Anyhow, hydrogen decreases temperature susceptibility of γ -TiAl alloys.

1.1.4 Effect of initial microstructures

Rheological characteristic of γ -TiAl alloys compressed at elevated temperature varies with microstructure characteristics (such as morphology and size)^[37] due to the difference in activated slip systems. Fig.6a contrasts the flow stress-strain curves during isothermal compression of Ti-49Al with different microstructures (fully lamellar FL and near gamma NG). As presented in Fig.6a, flow softening emerges in Ti-49Al with a NG microstructure, while flow behavior of Ti-49Al with a FL microstructure shows continual work hardening. The above phenomenon is related to the interactions between ordinary dislocation $1/2\langle[110]\rangle$, twin partial dislocations $1/6\langle[112]\rangle$ and lamellar interface. For γ -TiAl alloy with a FL microstructure, there is an exponential relationship between peak stress (or steady stress) and sizes of lamellar colony^[38].

Meanwhile, γ -TiAl alloys with different casting texture have different deformation responses to hot deformation processing parameters. Fig.6b presents the effect of original casting texture on high temperature deformation behavior of Ti-48Al-2Cr. As shown in Fig.6b, the effect of work hardening and flow softening on lamellar structure that is parallel to the compression direction is more obvious than in other directions, which can be explained below^[29]. The dislocation slipping and twinning in hard lamellae ($\alpha=0^\circ$ and $\alpha=90^\circ$) are restricted by lamellae interface, which leads to stress concentration in the vicinity of lamellae interface. Consequently, DRX is extensively stimulated, which results in flow softening. As for soft lamellae ($\alpha=45^\circ$), dislocation slipping is unimpeded. Thus, little dislocation pile-up occurs, which results in insufficient flow softening induced by DRX.

1.2 Kinetic analysis of hot deformation behavior

Apparent deformation activation energy Q , strain rate sensitivity index m and strain hardening index n are important indicators to measure high temperature deformation behavior of metals and alloys. Additionally, they reflect difficulty and uniformity of deformation. Kinetic analysis of γ -TiAl alloys is beneficial for accurately controlling forging process and quality of forming parts.

1.2.1 Apparent deformation activation energy

Physical nature of hot deformation for γ -TiAl alloys is atoms immigration. The energy needed for hot deformation is apparent deformation activation energy Q

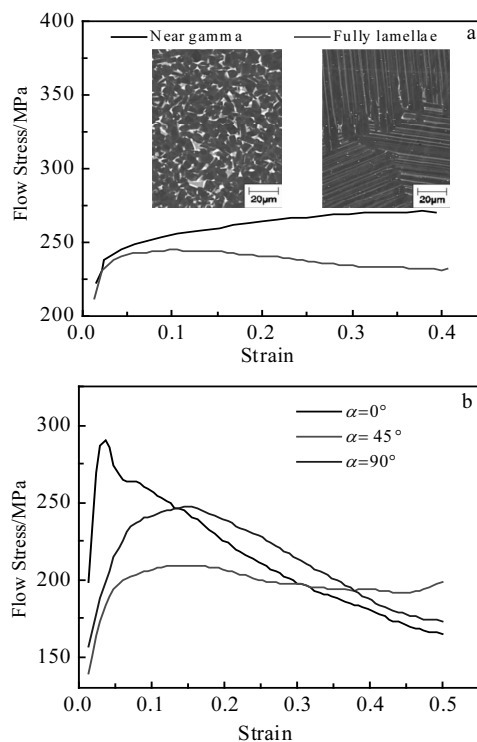


Fig.6 Effect of initial microstructure (a) (the illustrations are SEM-BSE images^[29]) and texture (b) on the flow stress-strain curves of γ -TiAl alloys (α represents the angle between lamellar interfaces and compression direction which is vertical^[29])

$$(Q = R \frac{d \ln \dot{\epsilon}}{d \ln \sigma} \Big|_{\epsilon, T} \frac{d \ln \sigma}{d \ln(1/T)} \Big|_{\dot{\epsilon}}),$$

which reflects the difficulty of hot deformation. Table 1 lists the apparent deformation activation energy Q and stress exponent n_1 of γ -TiAl alloys deformed under various processing parameters. As shown in Table 1, the Q value of γ -TiAl alloys ranges from 200 kJ·mol⁻¹ to 632 kJ·mol⁻¹. If the apparent deformation activation energy is equal to self-diffusion energy of Ti atom or Al atom, softening mechanism of γ -TiAl alloys is controlled by dislocation climbs, indicating that DRV is the primary flow softening mechanism. Otherwise, the high Q value is attributed to the DRX in γ -TiAl alloys.

Usually, influencing factors of flow behavior are same as those of activation parameters when γ -TiAl alloys are deformed at elevated temperature. As presented in Fig.7, apparent deformation activation energy declines with increasing the deformation temperature. However, apparent deformation activation energy possesses a peak value as strain increases. Besides, with increasing the fraction of β/β_0 phase, apparent deformation activation energy of γ -TiAl alloys decreases^[44]. Chen et al^[36] claimed that a trace of hydrogen

Table 1 Activation parameters of various γ -TiAl alloys (apparent deformation activation energy Q and stress exponent n_1)

γ -TiAl alloys	Initial microstructure	$T/^\circ\text{C}$	$\dot{\epsilon} / \text{s}^{-1}$	$Q/\text{kJ}\cdot\text{mol}^{-1}$	n_1
Ti-44Al-6Nb ^[36]	Fully lamellar	1100~1250	0.001~1.0	485.7	4.4
Ti-43Al-4Nb-1Mo-0.1B ^[39]	Nearly lamellar	1150~1300	0.005~0.5	200~350	3~4.5
Ti-41Al-3Mo-0.5Si-0.1B ^[40]	$\gamma+\beta$	1150~1300	0.005~0.5	267	2.95
Ti-45Al-3Mo-0.5Si-0.1B ^[40]	$\gamma+\beta$	1150~1300	0.005~0.5	553	
Ti-46.2Al-2V-1Cr-0.5Ni ^[41]	Nearly lamellar	950~1050	0.01~1.0	247	8.34
Ti-47Al-2Cr-0.2Mo ^[42]	Nearly γ	1000~1150	0.001~1.0	313.5	3.03
Ti-42Al-8Nb-0.2W-0.1Y ^[19]	$\gamma+\beta$	1000~1150	0.001~0.5	427	4.16
Ti-44Al-5V-1Cr ^[43]	Nearly lamellar	1000~1250	0.001~1.0	632	3.4

apparently reduces deformation activation energy of γ -TiAl alloys by about 21.2%, which indicates the improved workability γ -TiAl alloys due to β/β_0 phase.

1.2.2 Strain rate sensitivity index

Strain rate sensitivity index m ($m = \frac{d \ln \sigma}{d \ln \dot{\epsilon}}|_{\epsilon, T}$) reflects

contribution of grain sliding to deformation, namely, the base for estimating plastic deformation ability. Only superplastic deformation mechanism can be activated in γ -TiAl alloys when m is greater than 0.5^[26]. Zhang^[41] announced that the strain rate sensitivity index m is 0.12~0.13 when Ti-46.2Al-2V-1Cr-0.5Ni is compressed at a deformation temperature of 1100 °C.

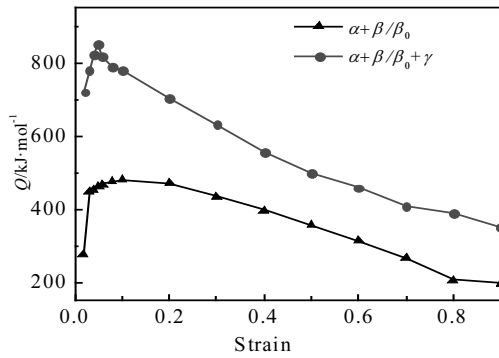


Fig.7 Effect of deformation temperature and strain on activation energy Q of Ti-43Al-4Nb-1Mo-0.1B^[39]

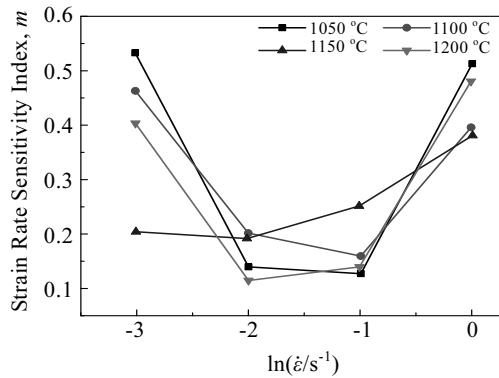


Fig.8 Effect of deformation temperature and strain on strain rate sensitivity index m of Ti-46Al-2V-1Cr-0.3Ni^[17]

As presented in Fig.8, most strain rate sensitivity index m of flow stress in γ -TiAl alloys first increases and then decreases with increasing the strain rate. Influence of deformation temperature on strain rate sensitivity index m is slightly complicated.

1.2.3 Strain hardening index and stress exponent

Strain hardening index n ($n = \frac{d \ln \sigma}{d \ln \epsilon}|_{\dot{\epsilon}, T}$) reflects strain dependence of flow stress. Variation of strain hardening exponent implies offset between work hardening and flow softening in γ -TiAl alloys deformed at different temperatures. Usually, strain hardening index n is a negative value.

Unlike the strain hardening index n , stress exponent n_1 reflects the deformation mechanism of γ -TiAl alloys, which can be calculated as $n_1 = \frac{d(\ln \dot{\epsilon} + Q/RT)}{d[\sinh(\alpha\sigma)]}$. As presented in

Table 1, stress exponent of γ -TiAl alloys ranges from 2.95 to 8.34. The lower the stress exponent, the bigger the contribution of grain sliding to deformation^[26]. As shown in Fig.9, similar to apparent deformation activation energy Q , stress exponent n_1 decreases with increasing the deformation temperature. However, when strain is lower than 10%, the change of stress exponent n_1 displays a contrary trend to that of apparent deformation activation energy. The stress exponent decreases very fast at the initial stage but then much slow. With increasing the strain, fine grains are formed and then grow up via deformation splintering and DRX, and thus the

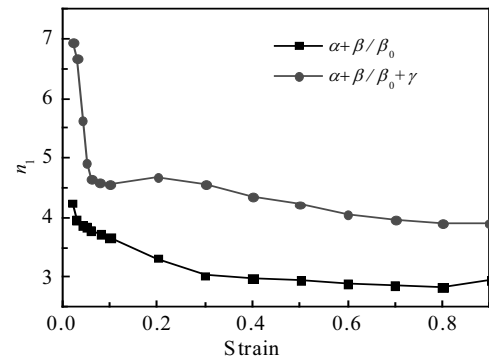


Fig.9 Effect of deformation temperature and strain on stress exponent n_1 of Ti-43Al-4Nb-1Mo-0.1B^[39]

contribution of grain sliding to plastic deformation of γ -TiAl alloys continuously decreases.

2 Constitutive Models of Flow Behavior of γ -TiAl Alloys

Constitutive models reflect mathematical relations between flow stress and hot deformation processing parameters (deformation temperature, strain rate and strain). Finite element modelling (FEM) software using a precise mathematical model has many benefits. First, it helps to obtain strain field and temperature field in γ -TiAl alloys deformed at elevated temperature. Meanwhile, prediction accuracy of actual deformation process is improved. By precise FEM simulation, industrial production costs of γ -TiAl alloys are effectively reduced. Based on mechanics and physics of plastic forming, Appel et al^[1] summarized modeling of transformation mechanisms and deformation mechanisms in γ -TiAl alloys. Zhang et al^[45] summarized the micro models and macro models of γ -TiAl alloys. They focus on constitutive models involving deformation mechanisms, in which practicality need to be improved. However, constitutive models considering flow softening mechanisms and microstructure evolution are neglected. Also, some empirical models with low computational complexity and high practicality, like H-S model, are neglected.

2.1 Empirical constitutive models

2.1.1 The Arrhenius model

The Arrhenius model^[46] is the most common constitutive model, which is expressed as follows:

$$\dot{\epsilon} = A[\sinh(\alpha\sigma)]^{n_1} \exp\left(-\frac{Q}{RT}\right) \quad (1)$$

where $\dot{\epsilon}$ is the strain rate; A , α and n_1 are material constants; σ is the flow stress; T is the absolute deformation temperature; Q represents the apparent activation energy for deformation; R is universal gas constant.

The Arrhenius model is widely adopted to describe flow behavior of metals and alloys. The simple mathematical expressions make it convenient to obtain parameters. Besides, the model has an excellent reproduction in flow stress.

The Arrhenius model ignores effect of strain on flow stress, which would cause significant predicted errors of flow stress. Thus considering strain compensation, A , α and n_1 are expressed as polynomial functions^[47] or exponential functions^[47-49] of strain. He et al^[48] established an Arrhenius model involving strain compensation of Ti-45Al-8.5Nb. The maximum absolute relative error between the predicted flow stress and the actual flow stress is 9.83%. However, Arrhenius model cannot reveal microstructure evolution and deformation mechanisms.

2.1.2 H-S model

H-S model^[50] is also an empirical model describing flow stress of alloys. The form is described as follows:

$$\sigma = A_0 \left[\dot{\epsilon}^{m_2} \exp\left(\frac{m_4}{\epsilon}\right) (1+\epsilon)^{m_3} \exp(m_7 \epsilon) \right] \exp(m_1 S) \left[\left(\frac{\dot{\epsilon}}{\dot{\epsilon}_0}\right)^{m_5+m_8 S} \right] \quad (2)$$

where A_0 , m_1 , m_2 , m_3 , m_4 , m_5 , m_7 and m_8 are coefficients that indicate the effect of deformation processing parameters on flow stress; $\dot{\epsilon}_0$ is 1.0 s^{-1} ; S is the Celsius temperature.

Unlike the Arrhenius model, H-S model takes strain into account. H-S model exhibits a good prediction accuracy of flow behavior. Meanwhile, H-S model can be directly used in FEM software. As shown in Fig.10, both the Arrhenius model and the H-S model exhibit excellent prediction results. However, flow stress data calculated from the Arrhenius model is illogical, when strain is out of experimental range^[40].

The H-S model cannot be used for kinetic analysis of deformation behavior. Besides, all empirical models are exclusive of deformation mechanisms or softening mechanisms.

2.2 Constitutive model combined with softening mechanisms

As shown in Fig.4, DRV is the softening mechanism of γ -TiAl alloys at the initial stage of deformation, while DRX becomes the primary softening mechanism after flow stress peaked. In this part, constitutive model combined with softening mechanisms is discussed in detail.

Laasraoui et al^[51] proposed a mathematical model by combining DRV with DRX. The model supposes that when strain is smaller than a critical strain ($\epsilon < \epsilon_p$), DRX will not occur and the flow stress can be calculated according to Eq.(3). When strain is larger than a critical strain ($\epsilon \geq \epsilon_p$), the flow stress can be calculated according to Eq.(4). Eq.(3) and (4) are defined as follows:

$$\sigma_{\text{dec}} = [\sigma_{\text{drv}}^2 + (\sigma_0^2 - \sigma_{\text{drv}}^2) e^{-Q\epsilon}]^{0.5} \quad (\epsilon < \epsilon_p) \quad (3)$$

$$\sigma = \sigma_{\text{dec}} - [\sigma_{\text{drv}} - \sigma_{\text{drx}}] \cdot \left\{ 1 - \exp\left[-K \left(\frac{\epsilon - \epsilon_p}{\epsilon_{0.5} - \epsilon_p}\right)\right] \right\} \quad (\epsilon \geq \epsilon_p) \quad (4)$$

where σ_{dec} is the flow stress before DRX occurs, σ_{drv} is the saturation stress when DRV is the exclusive softening mechanism, σ_{drx} is the flow stress when DRX is accomplished, σ_0 is the initial flow stress, Q is the coefficient of DRV, ϵ_p is the critical strain when DRX occurs, K is the material constant, and $\epsilon_{0.5}$ is the strain when DRX is half finished.

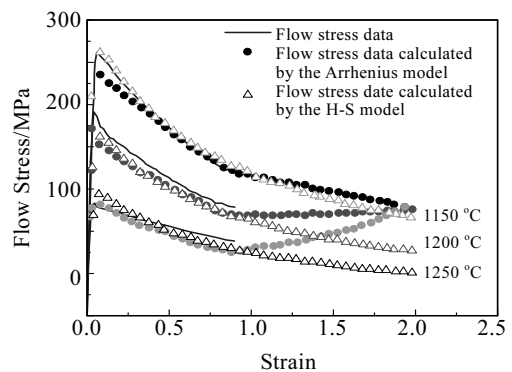


Fig.10 Comparison of actual flow stress and predicted flow stress of Ti-45Al-3Mo (strain rate of 0.5 s^{-1})^[40]

Compared with empirical models, this model coupled with different softening mechanisms can be used to describe flow stress of overall deformation. Contribution of DRV to flow stress can be quantitated by this model. Fig.11 shows the comparison between experimental flow stress and predicted flow stress by above mentioned constitutive model of Ti-42Al-8Nb^[14]. As shown in Fig.11, this constitutive model has a good prediction of flow stress. However, this model related to DRX is one-sided for revealing microstructure evolution in isothermal compression. Usually, the kinking of lamellae and spheroidization is often observed in isothermally compressed γ -TiAl alloys, which are omitted in Eq.(3) and (4).

2.3 Constitutive model coupling deformation mechanisms

2.3.1 Z-A model

Forms of Z-A model depend on crystal structure which is related to deformation mechanisms. The Z-A model is given as follows:

$$\sigma = C_0 + C_1 \varepsilon^{1/2} \exp[-C_2 T + C_3 T \ln(\frac{\dot{\varepsilon}}{\dot{\varepsilon}_0})] \text{ (fcc)} \quad (5)$$

$$\sigma = C_0 + C_4 \exp[-C_2 T + C_3 T \ln(\frac{\dot{\varepsilon}}{\dot{\varepsilon}_0}) + C_5 \varepsilon^b] \text{ (bcc)} \quad (6)$$

where $C_0, C_1, C_2, C_3, C_4, C_5$ and b are material constants, and other letters have the same meanings as mentioned above.

Based on deformation mechanisms (dislocation motion) of γ -TiAl alloys, Zan^[52] established a Z-A model with bcc structure, which possesses a good reproduction of rheological behaviors. However, deformation mechanisms are not completely involved in this model. Also, the parameters are difficult to ascertain, and thus prediction accuracy of Z-A model is lower than that of empirical models.

2.3.2 Other constitutive models involving deformation mechanisms

Appel et al^[1, 23, 53] proposed that during the deformation of γ -TiAl alloys, the flow stress is composed of athermal stress and thermal stress. Athermal stress is part of flow stress

caused by grain boundaries and phase interfaces. Thermal stress is caused by dislocation dipole and debris, which is sensitive to deformation temperature and strain rate. This model is presented as follows:

$$\sigma = \sigma_{\mu} + \sigma^*(\varepsilon) = \sigma_{\mu} + \frac{M_T}{V_d(\varepsilon)} \cdot [\Delta F + kT \ln(\frac{\dot{\varepsilon}}{\dot{\varepsilon}_0})] \quad (7)$$

where σ_{μ} is the athermal stress, $\sigma^*(\varepsilon)$ is the flow stress which is sensitive to deformation processing parameters, M_T is the Taylor factor, ΔF and V_d are the activation enthalpy and activation volume related to deformation mechanisms, respectively, k is the Boltzmann constant, and remaining letters' meanings are unchangeable. Usually, this model is used to ascertain mechanisms of dislocation motion at different temperatures, by virtue of V_d and apparent activation energy for deformation^[54].

There are many other models involving deformation mechanisms and nano-scale structure, which are detailed in Ref.[1, 45]. Because of the difficulty in parameters determination and poor practicability, these models are not reiterated here.

3 Conclusions and Prospects

Deformation behavior of γ -TiAl alloys compressed at elevated temperature is affected by many factors, such as increasing the deformation temperature, reducing the strain rate, suitable preheating treatment, moderate addition of certain elements, thermo-hydrogen treatment and designed microstructure, all of which are beneficial to reducing deformation resistance and improving deformation uniformity.

Constitutive models of γ -TiAl alloys can be divided into three groups: empirical models, models with different softening mechanisms and models involving deformation mechanisms. Empirical constitutive models have higher prediction accuracy. Although it is easy to determine parameters in empirical models, their physical meanings are ambiguous. Models including deformation mechanisms are conducive to understanding high temperature deformation behavior of γ -TiAl alloys from a micro perspective. However, parameters in the models are usually difficult to determine, which reduces the reliability of subsequent numerical simulation results.

In order to improve reliability of constitutive models, further research ought to get a deep comprehension concerning effect of microstructure and deformation mechanisms on flow behavior of γ -TiAl alloys.

In one way, the influence of α_2 grain and β/β_0 phase on flow stress of γ -TiAl alloys should be understood, and relevant microstructure features should be considered into constitutive models. γ -TiAl alloys consist of γ (TiAl) phase with L1₀ structure, α_2 (Ti₃Al) phase with D0₁₉ structure and β/β_0 phase with B2 structure. γ phase is the recognized majority during hot deformation. There are two types of γ

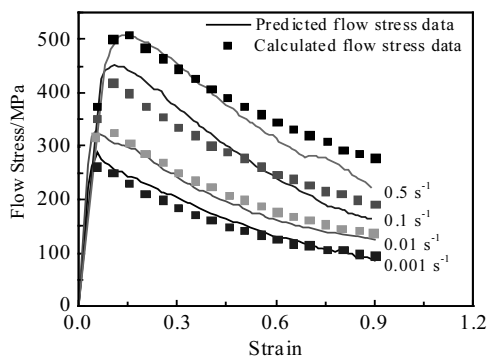


Fig.11 Comparison between predicted flow stress and experimental flow stress of Ti-42Al-8Nb (deformation temperature of 1050 °C)^[14]

phase: γ grain and γ lamellae. Deformation mechanisms vary with characteristics of γ phase. Besides, γ grain size and γ lamellae thickness are vital parameters, which have great effect on deformation behavior^[55, 56]. Unfortunately, problems mentioned above are ignored during derivation of constitutive models. As Qiu et al^[57] said, β/β_0 phase has various effects on deformation behaviors, such as lubrication effect and coordination effect. However, contribution of β/β_0 phase to hot deformation is neglected. Also, volume fraction, grain size and other characteristic parameters describing α_2 phase are omitted.

In the other way, it is important to deeply figure out the deformation mechanisms during hot compression of γ -TiAl alloys, and then to propose constitutive models involving multiphase coordinated deformation mechanisms. Twinning is frequently observed in γ phase^[58-60]. However, constitutive models involving dislocation glide and twinning are rarely established. Meanwhile, there are four lamellar boundaries in γ -TiAl alloys^[61]. It's a big problem to maintain continuity of strain in plastic forming. Interaction between γ phase, β/β_0 phase and α_2 phase is a significant factor which will influence deformation behavior of alloys. However, few theories can be found to describe and explain this factor. Moreover, constitutive models always ignore interaction between different phases. Thus, theories should be established to explain this interaction.

References

- Appel F, Clemens H, Fischer F D. *Progress in Materials Science*[J], 2016, 81:55
- Appel F, Wagner R. *Materials Science and Engineering R-Reports*[J], 1998, 22(5): 187
- Bewlay B P, Nag S, Suzuki A et al. *Materials at High Temperatures*[J], 2016, 33(4-5): 549
- Bewlay B P, Weimer M, Kelly T et al. *Mrs Proceedings*[J], 2013, 1516: 49
- Guyon J, Hazotte A, Wagner F et al. *Acta Materialia*[J], 2016, 103: 672
- Song Xiaojie, Cui Hongzhi, Hou Nan et al. *Ceramics International*[J], 2016, 42(12): 13 586
- Yamaguchi M, Inui H, Ito K. *Acta Materialia*[J], 2000, 48(1):307
- Clemens H, Mayer S. *Advanced Engineering Materials*[J], 2013, 15(4): 191
- Clemens H, Mayer S. *Materials at High Temperatures*[J], 2016, 33(4-5): 560
- Mayer S, Erdely P, Fischer F D et al. *Advanced Engineering Materials*[J], 2017, 19(4): 1 600 735
- Kartavykh A V, Asnis E A, Piskun N V et al. *Materials Letters*[J], 2016, 162: 180
- Janschek P. *Materials Today Proceedings*[J], 2015, 2: S92
- Seetharaman V, Semiatin S L. *Metallurgical and Materials Transactions A*[J], 1996, 27(7): 1987
- Cheng Liang, Xue Xiangyi, Tang Bin et al. *Intermetallics*[J], 2014, 49: 23
- Goetz R L, Semiatin S L. *Journal of Materials Engineering and Performance*[J], 2001, 10(6): 710
- Xin Jingjing, Zhang Laiqi, Ge Gengwu et al. *Materials and Design*[J], 2016, 107: 406
- Wen Daoshen, Zong Yingying, Wang Yaoqi et al. *Materials Science and Engineering A*[J], 2016, 656: 151
- Wan Zhipeng, Sun Yu, Hu Lianxi et al. *Materials Characterization*[J], 2017, 130: 25
- Cheng Liang, Chang Hui, Tang Bin et al. *Journal of Alloys and Compounds*[J], 2013, 552: 363
- Zhang W J, Lorenz U, Appel F. *Acta Materialia*[J], 2000, 48(11): 2803
- Huber D, Werner R, Clemens H et al. *Materials Characterization*[J], 2015, 109: 116
- Appel F, Herrmann D, Fischer F D et al. *International Journal of Plasticity*[J], 2013, 42: 83
- Paul J D H, Appel F. *Metallurgical and Materials Transactions A*[J], 2003, 34(10): 2103
- Sun Wei. *Thesis for Doctorate*[D]. Shenyang: Institute of Metal Research, Chinese Academy of Sciences, 2009 (in Chinese)
- Huang Z H. *Intermetallics*[J], 2005, 13(3): 245
- Appel F, Paul J D H, Oehring M. *Gamma Titanium Aluminide Alloys: Science and Technology*[M]. Weinheim: Wiley-VCH, 2011
- Clemens H, Wallgram W, Kremmer S et al. *Advanced Engineering Materials*[J], 2008, 10(8): 707
- Qiu Congzhang, Liu Yong, Huang Lan et al. *Transactions of Nonferrous Metals Society of China*[J], 2012, 22(11): 2593
- Imayev R M, Imayev V M, Oehring M et al. *Metallurgical and Materials Transactions A*[J], 2005, 36(3): 859
- Paul J D H, Appel F, Wagner R. *Acta Materialia*[J], 1998, 46(4): 1075
- Zhu Hanliang, Seo D Y, Maruyama K. *Jom*[J], 2010, 62(1): 64
- Cui Ning, Wang Xiaopeng, Kong Fantao et al. *Rare Metals*[J], 2016, 35(1): 42
- Appel F, Oehring M, Wagner R. *Intermetallics*[J], 2000, 8(9-11): 1283
- Huang Baiyun. *Intermetallics of Titanium Aluminides*[M]. Changsha: Central South University of Technology Press, 1998 (in Chinese)
- Nazarova T I, Imayev V M, Imayev R M et al. *Intermetallics*[J], 2017, 82: 26
- Chen Ruirun, Ma Tengfei, Guo Jingjie et al. *Materials and Design*[J], 2016, 108: 259
- Wang D J, Zhang R, Yuan H et al. *JOM*[J], 2017, 69(10): 1824
- Seetharaman V, Semiatin S L. *Metallurgical and Materials Transactions A*[J], 2002, 33(12): 3817
- Schwaighofer E, Clemens H, Lindemann J et al. *Materials Science and Engineering A*[J], 2014, 614: 297
- Godor F, Werner R, Lindemann J et al. *Materials Science and*

- Engineering A*[J], 2015, 648: 208
- 41 Zhang Ji, Zhang Zhihong, Su Xi et al. *Intermetallics*[J], 2000, 8(4): 321
- 42 Zhang Wei, Liu Yong, Li Huizhong et al. *Journal of Materials Processing Technology*[J], 2009, 209(12-13): 5363
- 43 Liu Hongwu, Rong Rong, Gao Fan et al. *Metals*[J], 2016, 6(12): 305
- 44 Zhang Hao. *Thesis for Doctorate*[D]. Harbin: Harbin Institute of Technology, 2010 (in Chinese)
- 45 Zhang Hongjian, Wen Weidong, Cui Haitao. *Materials for Mechanical Engineering*[J], 2013, 37(7): 1 (in Chinese)
- 46 Sellars C M, McTegart W J. *Acta Metallurgica*[J], 1966, 14(9): 1136
- 47 Liang Xiaopeng, Liu Yong, Li Huizhong et al. *Materials and Design*[J], 2012, 37: 40
- 48 He Xiaoming, Yu Zhongqi, Liu Guiming et al. *Materials and Design*[J], 2009, 30(1): 166
- 49 Sun Yu, Hu Lianxi, Ren Junshuai. *Journal of Materials Engineering and Performance*[J], 2015, 24(3): 1313
- 50 Hensel A, Spittel T. *Kraft-Und Arbeitsbedarf Bildsamer Formgebungsverfahren*[M]. Leipzig: VEB Deutscher Verlag für Grundstoffindustrie, 1978
- 51 Laasraoui A, Jonas J J. *Metallurgical Transactions A*[J], 1991, 22(7): 1545
- 52 Zan Xiang. *Thesis for Doctorate*[D]. Hefei: University of Science and Technology of China, 2008 (in Chinese)
- 53 Appel F, Wagner R. *Materials Science and Engineering R Reports*[J], 1998, 22(5): 187
- 54 Leyens C, Peters M. *Titanium and Titanium Alloys*[M]. Weinheim: Wiley-VCH, 2003
- 55 Kim H Y, Maruyama K. *Acta Materialia*[J], 2003, 51(8): 2191
- 56 Kanani M, Hartmaier A, Janisch R. *Acta Materialia*[J], 2016, 106: 208
- 57 Qiu Congzhang, Liu Yong, Huang Lan et al. *Transactions of Nonferrous Metals Society of China*[J], 2012, 22(11): 2593
- 58 Kim J H, Shin D H, Semiatin S L et al. *Materials Science and Engineering A*[J], 2003, 344(1-2): 146
- 59 Cerreta E, Mahajan S. *Acta Materialia*[J], 2001, 49(18): 3803
- 60 Marketz W T, Fischer F D, Clemens H. *International Journal of Plasticity*[J], 2003, 19(3): 281
- 61 Nakano T, Nakai Y, Umakoshi Y. *Science and Technology of Advanced Materials*[J], 2002, 3(2): 225

γ -TiAl 合金高温塑性变形力学行为及本构模型的研究进展

胥润润, 李淼泉, 李宏

(西北工业大学, 陕西 西安 710072)

摘要: 轻质高强 γ -TiAl 合金是航空发动机关键结构件减重的首选材料。概括总结了 γ -TiAl 合金的高温压缩变形力学行为及本构模型, 重点分析了变形工艺参数、变形历史和预热处理、元素、原始组织对 γ -TiAl 合金高温压缩变形力学行为的影响。本文概括了 3 种本构模型: 经验型本构模型、不同软化机制下的本构模型和耦合变形机理的微观模型, 并对 Arrhenius 模型和 H-S 模型进行了详细分析。同时, 对不同软化机制下的本构模型和耦合变形机理的模型进行了总结分析。最后指出, γ -TiAl 合金高温压缩变形力学行为的未来研究重点是建立耦合多相协调性高温变形机理的本构模型。

关键词: γ -TiAl 合金; 高温变形; 动力学分析; 本构模型

作者简介: 胥润润, 女, 1993 年生, 博士生, 西北工业大学材料学院, 陕西 西安 710072, 电话: 029-88460328, E-mail: runrunru@126.com